



Research paper

Comparison of analytical methods to detect instability of etanercept during thermal stress testing

Andreas van Maarschalkerweerd^a, Gert-Jan Wolbink^b, Steven O. Stapel^b, Wim Jiskoot^a, Andrea Hawe^{a,*}^a Division of Drug Delivery Technology, Leiden University, Leiden, The Netherlands^b Sanquin Research, Amsterdam, The Netherlands

ARTICLE INFO

Article history:

Available online 24 January 2011

Keywords:

Aggregation

Extrinsic fluorescence

Bis-ANS

Enbrel

Protein stability

Conformational changes

ABSTRACT

The aim was comparing the capability of a set of analytical methods to detect physical instability (focus on aggregation and structural changes) of etanercept during thermal stress testing as early as possible. Pre-filled syringes of Enbrel[®] 50 mg from three batches were thermally stressed for one week at 50 °C. Samples were taken at days 0, 1, 2, 3, 4 and 7, and analyzed with high-performance liquid size exclusion chromatography (HP-SEC), SDS-PAGE gel electrophoresis, dynamic light scattering (DLS), light obscuration, extrinsic fluorescence (Bis-ANS), far-UV circular dichroism (CD) spectroscopy, second derivative UV spectroscopy (UV), and enzyme-linked immunosorbent assay (ELISA). Thermal stress resulted in the formation of small soluble aggregates (HP-SEC, DLS) which were in part covalent (SDS-PAGE), and conformationally changed (Bis-ANS, CD, UV). No significant increase in subvisible particles was detected by light obscuration. An apparent increase in TNF- α binding to etanercept in the stressed formulations was found by ELISA. The three batches were comparable when unstressed, but showed slight differences in aggregation tendency. Bis-ANS fluorescence was most sensitive with respect to early-stage detection of heat-induced instability of etanercept (significant changes already at day 1), followed by HP-SEC (day 2) and DLS (day 3). This points towards a degradation mechanism involving exposure of hydrophobic patches due to partial unfolding followed by aggregation.

© 2011 Elsevier B.V. All rights reserved.

1. Introduction

In recent years, protein pharmaceuticals have overtaken low molecular weight compounds within novel drug development [1,2]. Due to their complex structural properties and instability, assessment of the quality of protein pharmaceuticals requires extensive physico-chemical characterization. Both chemical degradation and physical degradation are important issues during the pharmaceutical development of therapeutic proteins [3]. Proteins are inclined to degrade and especially form aggregates as a result of external stress factors, such as temperature, mechanical stress, surface-induced denaturation or light exposure [4,5]. Protein aggregates are critical because of possible activity loss and immunogenicity concerns [6–8], as exemplified by insulin [9,10], human

growth hormone [11] and interferon-beta [12]. Aggregates can be considered as a heterogeneous group of protein assemblies, composed of a varying number of associated monomers, which can be native-like or conformationally changed. Depending on the applied stress, such as agitation, freeze-thawing, or heating, it is expected that aggregates with different characteristics are formed [13,14]. In order to gain a proper understanding of the characteristics of the protein and its aggregates, it is therefore essential to combine the results of a broad range of orthogonal analytical methods [13–15].

The standard method used to separate and quantify small soluble protein aggregates in solution is high-performance liquid size exclusion chromatography (HP-SEC). For the analysis of subvisible particles in the nanometer size range, dynamic light scattering (DLS) is commonly employed. DLS has the advantage of being very sensitive to small amounts of aggregates, but unlike HP-SEC, it is not suitable for quantification of aggregates. Light obscuration allows the quantification of particles in the micrometer size range. Despite being susceptible to measure small amounts of aggregates, these methods have their limitations [16,17] and are not capable to detect minute quantities of monomeric precursors of aggregation or subtle structural changes. For the analysis of such structurally changed species spectroscopic techniques, e.g. CD spectroscopy or fluorescence spectroscopy using extrinsic dyes, are available.

Abbreviations: HPE, high-performance ELISA buffer; TNF- α , tumor necrosis factor- α ; MRW, mean residue ellipticity; AUC, area under the curve; HMW, molecular weight species; Bis-ANS, 4,4'-dianilino-1,1'-binaphthyl-5,5'-disulfonic acid dipotassium salt; ELISA, enzyme-linked immunosorbent assay; DLS, dynamic light scattering; HP-SEC, high-performance liquid size exclusion chromatography; PDI, polydispersity index.

* Corresponding author. Address: Division of Drug Delivery Technology, Leiden/Amsterdam Center for Drug Research, Leiden University, P.O. Box 9502, 2300 RA Leiden, The Netherlands. Tel.: +31 71 527 4350.

E-mail address: ahawe@chem.leidenuniv.nl (A. Hawe).

The main aim of our study was comparing different analytical methods for their sensitivity to detect instability of etanercept (Enbrel®) during stress testing performed at 50 °C. A set of methods commonly used for protein stability testing, including HP-SEC, DLS, light obscuration, sodium dodecyl sulfate polyacrylamide gel electrophoresis (SDS–PAGE), fluorescence spectroscopy with the extrinsic dye Bis-ANS, second derivative UV spectroscopy, far-UV circular dichroism spectroscopy (far-UV CD) and enzyme-linked immunosorbent assay (ELISA), was included within the study. The focus of the analytical characterization was to set on aggregates of various types and sizes, as well as structural changes. Although being sensitive to different degradation products, a comparison of those methods is of high relevance, as it is common practice, e.g. during formulation development to use a combination of analytical methods to assess the stability of different formulations.

Etanercept is a fusion protein consisting of a human necrosis factor receptor (TNF- α) coupled to the Fc domain of human IgG1, which has been commercialized for the treatment of rheumatoid arthritis and psoriasis [18,19]. We monitored structural changes and aggregation of etanercept during thermal stress at 50 °C, which was below the melting temperature of the protein at about 68 °C. The selected stress conditions can be regarded as relevant for situations a protein could be exposed to, for example, for stress testing performed during the development of biopharmaceutical drugs or in real life situations like an accidental exposure to elevated temperature during transport. Our results demonstrate that extrinsic dye fluorescence using Bis-ANS was capable to detect instability of etanercept at an earlier stage than HP-SEC, DLS and the other techniques.

2. Materials and methods

2.1. Materials

The commercial product Enbrel® 50 mg (1 ml, containing 50 mg/ml etanercept) obtained from local hospitals was used as model drug for this study. Batch numbers 35082 (expiry date [ED] 02/2010, $n = 3$), 35561 (ED 03/2010, $n = 3$) and 33797 (ED 09/2009, $n = 3$) of Enbrel® 50 mg were used. The study was finalized around or up to 6 months after the expiry date. Chemicals used to prepare buffers were of analytical grade unless otherwise specified.

4,4'-Dianilino-1,1'-binaphthyl-5,5'-disulfonic acid dipotassium salt (Bis-ANS) from Sigma (Sigma-Aldrich, Steinheim, Germany) was applied as extrinsic fluorescent dye in this study. A stock solution of Bis-ANS was prepared in 99.9% (v/v) ethanol from Biosolve (Biosolve B.V., Valkenswaard, The Netherlands) at a concentration of 200 μM . Dye concentration was determined with UV spectroscopy after dilution with ethanol using a molar absorption coefficient of 21,120 $\text{M}^{-1} \text{cm}^{-1}$ at 397 nm in ethanol [20].

2.2. Stress testing of etanercept

The pre-filled Enbrel® 50 mg syringes were incubated in a stove at 50 °C. Aliquots of 80 μl were taken for the analysis before thermal stressing and after 1, 2, 3, 4 and 7 days at 50 °C. For the analytical characterization, the samples were diluted to 0.1 mg/ml in formulation placebo (ELISA), to 1.0 mg/ml in formulation placebo (for extrinsic dye fluorescence, HP-SEC, DLS, light obscuration, and SDS–PAGE) and to 0.25 mg/ml in MilliQ-water (for 2nd derivative UV and far-UV CD). MilliQ-water and formulation placebos were filtered through 0.22- μm PES low-binding syringe-driven filter units (Millex™ GP, Millipore, Ireland) before using them for the dilutions. All dilutions were prepared in a laminar flow cabinet. The formulation placebo contained 10 mg/ml sucrose (Fluka, Sigma Aldrich Steinheim, Germany), 5.8 mg/ml NaCl (Sigma, Sigma

Aldrich Steinheim, Germany), 5.3 mg/ml arginine hydrochloride Merck (Merck KGaA, Darmstadt, Germany, and 3.9 mg/ml $\text{Na}_2\text{H-PO}_4\cdot\text{H}_2\text{O}$ (Sigma, Sigma Aldrich, Steinheim, Germany) (pH 6.3).

2.3. HP-SEC

HP-SEC was performed with a Waters 515 pump, a Waters 717 plus autosampler, and a Waters 474 UV detector (Waters, Milford Massachusetts, USA). A TSKgel4000 SWXL column (300 \times 7.8 mm) (Tosoh Biosep, Stuttgart, Germany) was used. Fifty microliters of the formulations was injected, and separation was performed at a flow rate of 0.5 ml/min. The running buffer was composed of 50 mM phosphate, 150 mM arginine and 0.025% NaN_3 at pH 6.5. UV detection was performed at 280 nm. To calculate the protein recovery, the total area under the curve (AUC) of the UV signal at 280 nm of the stressed samples was compared with the total AUC of the non-stressed samples, which was set to 100%. The monomer content in% was calculated as the AUC of the monomer compared to the total AUC \times 100. Dimers and higher molecular weight species (HMW) were calculated accordingly.

2.4. SDS–PAGE

SDS–PAGE was performed using a vertical Bio-Rad Mini-Protean 3 gel electrophoresis system (Bio-Rad laboratories, Hercules, USA) under reducing (β -mercaptoethanol) and non-reducing conditions using 7.5% Tris–HCl Gels (Bio-Rad Laboratories, Hercules, USA). Five microliters of protein sample (1.0 mg/ml in formulation buffer) was added to each well after incubating (95 °C, 5 min) with 5 μl of sample buffer (Tris–HCl, glycerol, SDS, bromophenol blue; for reducing conditions with β -mercaptoethanol). A broad range molecular weight marker was used (Bio-Rad Laboratories, Hercules, USA). The gels were stained with Coomassie Blue.

2.5. Dynamic light scattering

DLS was performed with the Zetasizer Nano (Malvern, Herenberg, Germany) equipped with a 633-nm He–Ne laser. Protein samples with a concentration of 1.0 mg/ml in formulation placebo were measured in 1.5-ml semi-micro disposable cuvettes from Brand (Brand GMBH, Wertheim, Germany). Each sample was measured three times with 10 subruns of 10 s each. The Z-average diameter and the polydispersity index (PDI) were calculated from the correlation function using the Dispersion Technology Software (version 4.20, Malvern).

2.6. Light obscuration

Subvisible particles in a size range between 1 and 200 μm were measured by light obscuration (LO) using a SVSS-C with a HCB-LD-25/25 sensor (PAMAS, Partikelmess- und Analysensysteme GmbH, Rutesheim, Germany). Three measurements of a volume of 0.2 ml of each protein sample (1.0 mg/ml in formulation placebo) were taken with a pre-run volume of 0.3 ml at a fixed fill rate, emptying rate and rinse rate of 10 ml/min. Prior to each measurement, the system was rinsed with filtered MilliQ-water (0.22 μm syringe driven Millipore™ filter). Results were calculated as the total count of particles $\geq 1 \mu\text{m}$, $\geq 10 \mu\text{m}$ and $\geq 25 \mu\text{m}$ per ml. The results were corrected for the particle-counts measured in the formulation placebos used for dilution of the samples and for the dilution step itself.

2.7. Bis-ANS fluorescence

A Tecan Infinite M1000 platereader (Tecan Benelux BVBA, Gies-sen, The Netherlands) was used to measure the extrinsic fluorescence of Bis-ANS by top reading in black polypropylene 96-well

plates (Greiner Bio-One B.V., Alphen a/d Rijn, The Netherlands). One hundred microliters of protein sample (1.0 mg/ml) per well was mixed with 2.5 μ l Bis-ANS stock solution to achieve a Bis-ANS concentration of 5 μ M ($n = 3$). Each measurement was recorded within 5 min after addition of the dye. Bis-ANS was excited at 385 nm with emission scanned from 400 to 650 nm. The measurements were performed with slits of 5 nm, steps of 2 nm and flashes of 5 joules.

2.8. Far-UV CD spectroscopy

For far-UV CD spectroscopy, the protein samples diluted to 0.25 mg/ml with freshly filtered MilliQ-water were measured with a Jasco J-815 CD spectrometer in combination with a Jasco PTC-423S temperature controller (Jasco International, Tokyo, Japan) in quartz cuvettes (Hellma GmbH, Muehlheim, Germany) with a path length of 2 mm at 25 °C. Far-UV CD spectra were collected from 200 to 250 nm at a scanning speed of 100 nm/min, a response time of 2 s, a bandwidth of 1 nm, a sensitivity of 100 mdeg, steps of 0.5 nm and an accumulation of 8 scans. Using the Spectra Analysis Software (version 1.53.04, Jasco), the spectra were background corrected for the spectrum of the solvent (diluted formulation placebo). Data were calculated as mean residue ellipticity based on a mean amino acid residue weight of 113 assumed for etanercept [21,22]. The mean residue ellipticity was determined according to Kelly et al. (2005) as $[\theta]_{\text{mrw},\lambda} = (\text{MRW} * \theta_{\lambda}) / (10 * c * d)$, where MRW is the mean residue weight, θ_{λ} is the observed ellipticity in millidegrees at wavelength λ , c is the protein concentration in mg/ml and d is the path length in cm.

2.9. Second derivative UV spectroscopy

UV spectroscopy was measured using an Agilent 8453 UV-Vis spectrometer (Agilent Technologies, Waldbronn, Germany). The samples (0.25 mg/ml diluted in freshly filtered MilliQ-water) were measured in 2-ml half-micro quartz cuvettes (Hellma Benelux, Kruibeke, Belgium) with a path length of 10 mm. The absorbance was measured from 240 to 340 nm with intervals of 1 nm using an integration time of 15 s. Background correction was performed with formulation placebo, diluted accordingly in freshly filtered MilliQ-water. The second derivatives of the spectra were calculated with UV-Visible ChemStation Software (Agilent Technologies, Waldbronn, Germany) using a filter length of 9 nm and a polynomial degree of 4. Thereafter, the second derivatives were splined using 99 data points between the 1-nm measurement points.

Within the second derivatives, the a/b -ratio's were calculated as the difference in intensity of the 288-nm maximum and the 284-nm minimum peaks divided by the difference in intensity between the 296 nm maximum and the 291 nm minimum (for further description see Ragone et al. [23]). The a/b -ratio is a measure of the polarity of the tyrosyl microenvironment, which will become more polar following protein denaturation [23].

2.10. Enzyme-linked immunosorbent assay

Functional etanercept levels were assessed by ELISA, based on the principle that etanercept is captured through its ability to bind TNF- α (Sanquin, Diagnostic Services, Amsterdam, the Netherlands). The sensitivity of detection is 1 ng/ml [24]. A mouse monoclonal antibody directed against TNF- α (CLB TNF/5) was coated overnight at room temperature (0.2 μ g/well) on flat bottomed microtitre plates. Recombinant TNF- α (0.05 μ g/ml) (Strathmann Biotech GmbH, Hannover, Germany) in high-performance ELISA (HPE) buffer (Business Unit reagents, Sanquin, Amsterdam, The Netherlands) was added (5 ng/well) for 1 h incubation. After washing with phosphate-buffered saline/0.02% Tween-20, samples were

added in different dilutions HPE-buffer, and the plates were incubated for 1 h at 37 °C. Plates were washed with phosphate-buffered saline/0.04% Tween-20, and incubated with biotinylated polyclonal rabbit antibodies against etanercept in 100 μ l HPE-buffer for 1 h at 37 °C. Subsequently, after washing, poly-HRP-conjugated streptavidin (Sanquin, Amsterdam, the Netherlands) was added (30 min at 30 °C), and plates were developed by adding 100 μ l of HRP substrate solution (Uptima, France) per well and incubated for 30 min at 30 °C. The reaction was stopped by 100 μ l of H₂SO₄ per well; absorption at 450 nm was measured with a multiscan UV plate reader (Multiskan; Titertek, Elfab Oy, Finland), and results were related to a titration curve of etanercept, present in each plate.

2.11. Statistical analysis

To assess the sensitivity of the different methods to detect changes in the progress of the thermal stress study, statistical analysis of the data from day 1, 2, 3, 4 and 7 compared with those from day 0 (before stress was applied) was performed by one-way ANOVA with a post test (Tukey) with $\alpha = 0.05$ (95% confidence interval) using GraphPad Prism (Version 5.02). This was performed individually per batch (3 syringes per batch were analyzed) and for all batches together (total $n = 9$).

3. Results

3.1. High-performance size exclusion chromatography

Monomers, dimers, HMW compounds and fragments were quantified by HP-SEC, and the total AUC of the chromatograms was determined. From the integration of the HP-SEC chromatograms (Fig. 1A), a loss of monomer (Fig. 1B), an increase in dimers (Fig. 1C), HMW compounds (Fig. 1D), and fragments (data not shown) during stress testing of etanercept becomes obvious.

At t_0 , a monomer content of about 97% was found, and all three batches were comparable. Besides a low level of aggregates, a small fraction of fragments could be detected in the non-stressed products. The fragment content was subjected to some fluctuation during thermal stressing, but with no overall increase, leaving the fragment content at 1.2–1.5% at day 7.

A gradual loss of monomer was observed during the thermal stress testing, which was up to about 50% at day 7. Batch 33797 was found to be more prone to aggregation than the other two batches, with batch 35082 being the most stable one. The dimer content increased to an almost constant level of about 5% after day 4, as obvious from Fig. 1C. It is clear that aggregation was mainly manifested in the formation of HMW species (Fig. 1D).

The total AUC of the HP-SEC chromatograms remained constant during stress testing (data not shown), indicating that no significant losses due to insoluble aggregates or the formation of larger particles occurred.

3.2. SDS-PAGE gel electrophoresis

SDS-PAGE was performed to clarify whether the formed aggregates detected by HP-SEC were covalent or non-covalent. For the non-stressed formulations, a main band of the monomer at 150 kDa is seen, which is the expected size of etanercept [18]. In addition, a few faint bands deriving from fragments were detected (Fig. 2; non-reducing conditions). After 3 and 7 days of stressing (lanes 3 and 4), a band is found at the top of the gel under non-reducing conditions, pointing at the formation of aggregates. As this band is not present under reducing conditions (Fig. 2), it can be concluded that these aggregates are covalently linked via

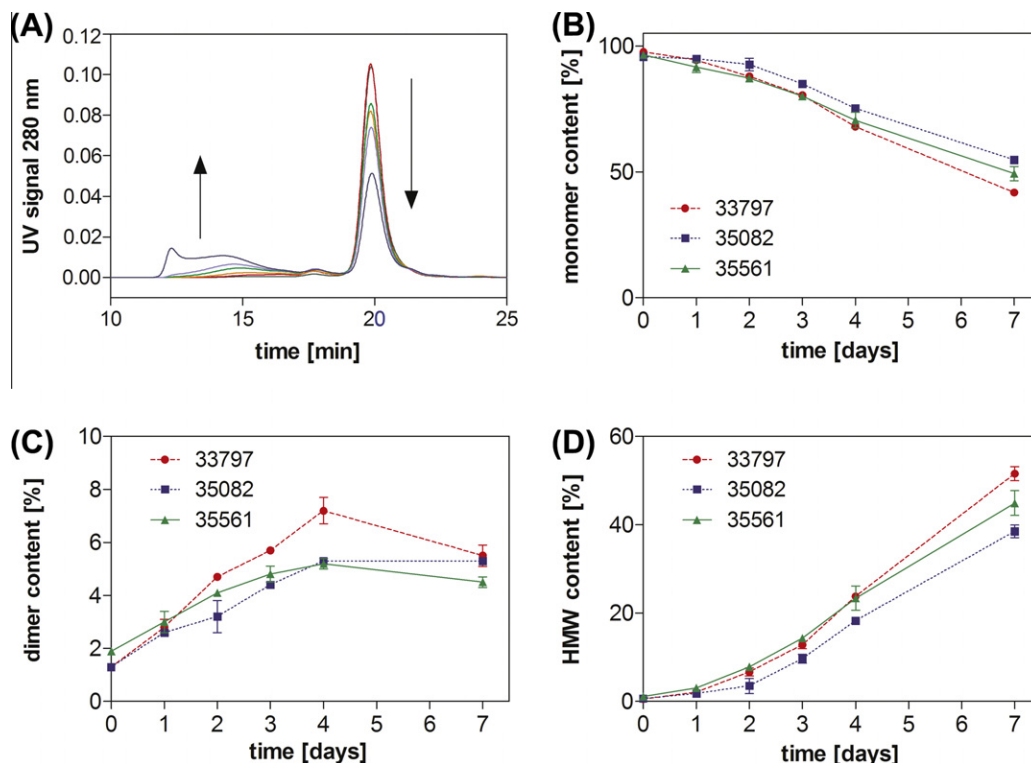


Fig. 1. HP-SEC chromatograms of batch 33797 (A), and monomer content (B), dimer content (C), and HMW content (D) of batches 33797, 35082, and 35561 in the progress of the stress study at 50 °C. (For interpretation of the references to color in this figure legend, the reader is referred to the web version of this article.)

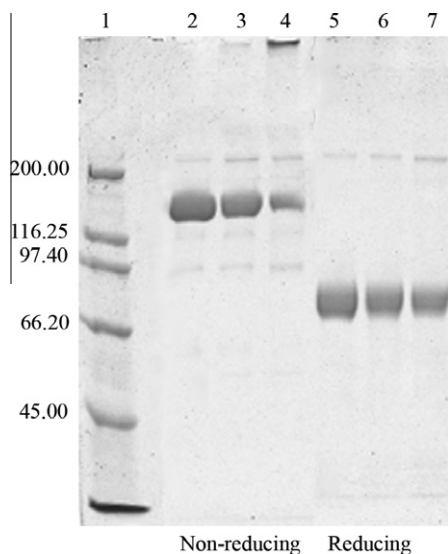


Fig. 2. SDS-PAGE of exemplary samples from batch 33797 under non-reducing (lanes 1–4) and reducing (lanes 5–7) conditions. Lane 1: marker, lanes 2 and 5: untreated, lanes 3 and 6: 3 days at 50 °C and lanes 4 and 7: 7 days at 50 °C.

disulfide bridges. Under reducing conditions, one band at about 70 kDa is found, deriving from the Fc-part and the TNF- α receptor, which have a similar molar mass of 75 kDa.

3.3. Dynamic light scattering

Dynamic light scattering (DLS) was used as a sensitive tool to detect small amounts of aggregates in the nanometer size range. The Z-average diameter of the unstressed etanercept was approximately 12.5 nm for all three tested batches (Fig. 3A) with a PDI of

about 0.1 (Fig. 3B). The Z-average diameter of all three batches increased only slightly within the first three days. Thereafter, the Z-average diameters increased more rapidly, which is a clear sign of aggregation. Batch 33797 was found to increase to higher Z-average values after 7 days than batches 35561 and 35082, confirming the stability trend obtained by HP-SEC.

The polydispersity index showed some fluctuation over time (Fig. 3B), with a trend to higher PDI values first after day 3. Compared to the increase in Z-average diameter, the PDI gave less clear results. Again all three batches were similar at t_0 with a PDI of 0.11, as expected for a predominantly monomeric solution. An increase in the PDI to approximately 0.15 was measured after 1–2 days of stressing, pointing to increased size heterogeneity due to the formation of aggregates [15].

3.4. Light obscuration

Light obscuration was applied to measure the content of subvisible particles larger than 1 μ m, 10 μ m and 25 μ m (Fig. 4A–C). No obvious changes in the particle count were observed within 7 days of thermal stressing. This is in agreement with the constant total AUC in HP-SEC. The formulations were within the limits of the requirement of the Ph. Eur. on low volume parenteral products [25]. Some fluctuations were observed during the stress testing, but only a slight tendency towards an increase in particle count could be seen (Fig. 4C) for the larger (>25 μ m) particles. For etanercept treated by thermal stress particle formation appeared to be not the prevalent aggregation mechanism. Therefore, light obscuration was not a suitable stability-indicating method for this particular application.

3.5. Bis-ANS fluorescence

The extrinsic non-covalent fluorescent dye Bis-ANS was employed to monitor conformational changes and aggregation of

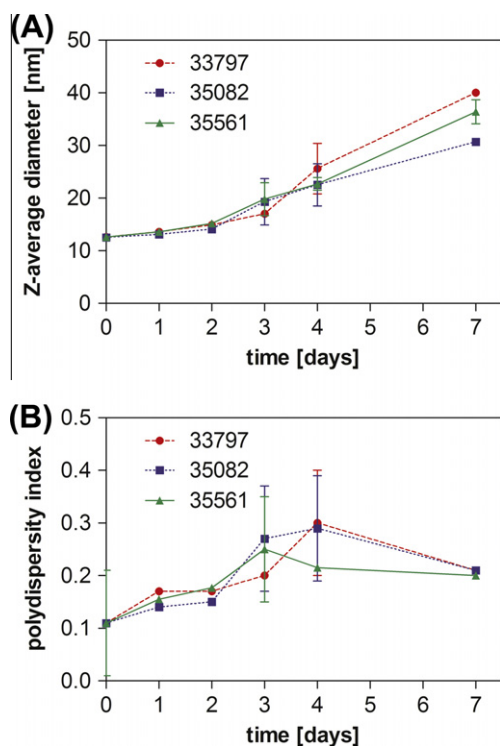


Fig. 3. Z-average diameter (A) and polydispersity index (B) of batches 33797, 35082, and 35561 in the progress of the stress study at 50 °C. (For interpretation of the references to color in this figure legend, the reader is referred to the web version of this article.)

etanercept. The dye was added to aliquots of the etanercept samples (after they were cooled down) at the different time-points during the accelerated stress study. Fig. 5A shows the spectral changes of Bis-ANS fluorescence emission, exemplarily for batch 33797. Already after 24 h, an increase to nearly 250% of the original fluorescence intensity (at the emission maximum of 492 nm) was observed, which was followed by a steady increase throughout the experiment.

Fig. 5B shows the development in maximum Bis-ANS fluorescence intensity (at 492 nm) for batches 33797, 35082, and 35561 during stress testing. At t_0 , all batches showed comparably low dye fluorescence, indicating strong similarity of the protein's conformational state and structure. This was followed by a steady increase in fluorescence clearly detectable already after 24 h. Batch 33797 underwent changes more rapidly than batches 35082 and 35561, despite comparable starting levels. This is consistent with the observations made by HP-SEC and DLS.

3.6. Far-UV CD spectroscopy

Far-UV CD spectroscopy was used to monitor changes in secondary structure. Because of the characteristic signals related to α -helix, anti-parallel β -sheets, and parallel β -sheets, changes in the far-UV CD signal can be related to certain secondary structure elements [26]. For aggregates composed of non-native monomers, a change of the CD spectrum may be expected. The spectra of non-stressed and thermally stressed etanercept are exemplarily depicted in Fig. 6A for batch 33797. The far-UV CD spectra were dominated by a local maximum of negative ellipticity at approximately 223 nm and a local minimum of negative ellipticity at approximately 230 nm. To follow the spectral changes during the accelerated stress study, the results of the tested batches are depicted as the average of the local maximum region from 222 to 224 nm

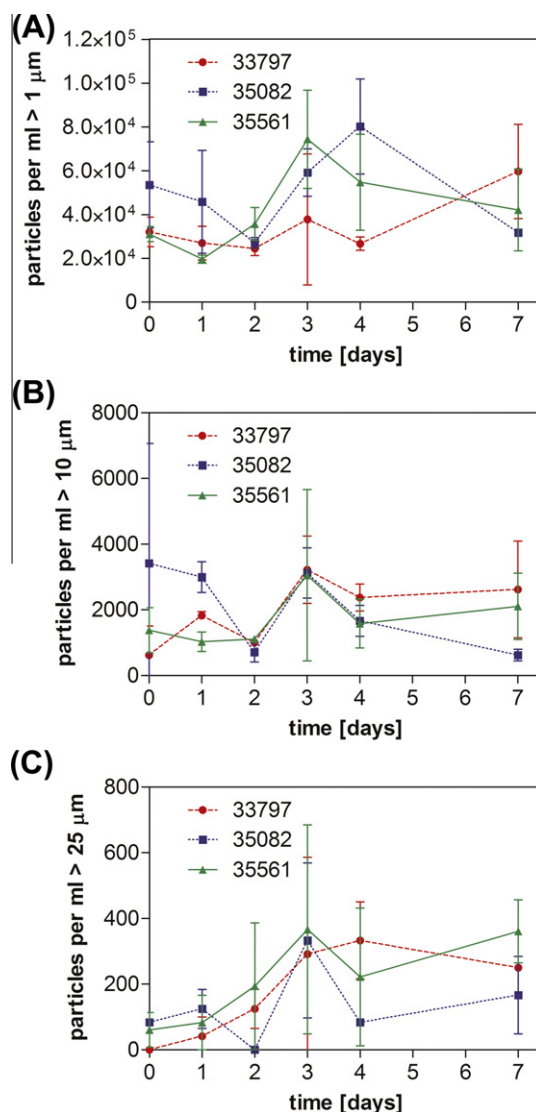


Fig. 4. Light obscuration results showing the particle count per ml of particles >1 μm (A), >10 μm (B), and >25 μm (C) of batches 33797, 35082, and 35561 in the progress of the stress study at 50 °C. (For interpretation of the references to color in this figure legend, the reader is referred to the web version of this article.)

(Fig. 6B). A gradual increase in the negative values was measured during the stress study, pointing at structural changes of the protein. However, it was not possible to discriminate between the different batches included in the study.

3.7. Second derivative UV spectroscopy

Conformational changes of the etanercept molecules were monitored by second derivative UV spectroscopy. Previous studies from the literature have shown that blue-shifts in peak positions can be attributed to an increase in the polarity of the local environment of tryptophan, tyrosine and phenylalanine [23,27,28]. Fig. 7A shows the collected second derivative UV absorption spectra exemplarily for batch 33797. The largest shifts for etanercept were only about 0.05 nm without a clear time-dependent trend (results not shown) and therefore not stability indicating.

In addition to the peak position, the relative peak intensities have been compared as the a/b -ratio to describe changes in the exposure of the tyrosine residues [23]. No early structural changes were observed with 2nd derivative UV between day 1 and 4 of the

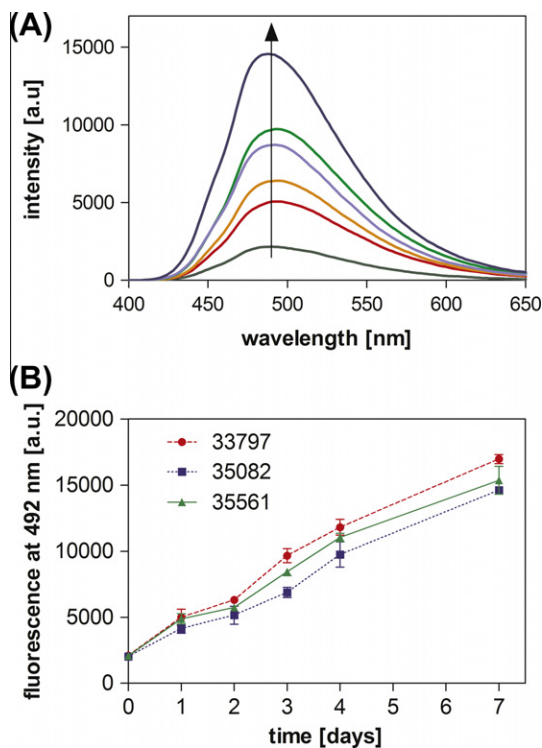


Fig. 5. Bis-ANS fluorescence spectra of batch 33797 (excitation at 385 nm, 1 μ M Bis-ANS) (A) and maximum extrinsic dye fluorescence recorded at 492 nm of batches 33797, 35082, and 35561 (B) in the progress of the stress study at 50 °C. a.u. arbitrary units. (For interpretation of the references to color in this figure legend, the reader is referred to the web version of this article.)

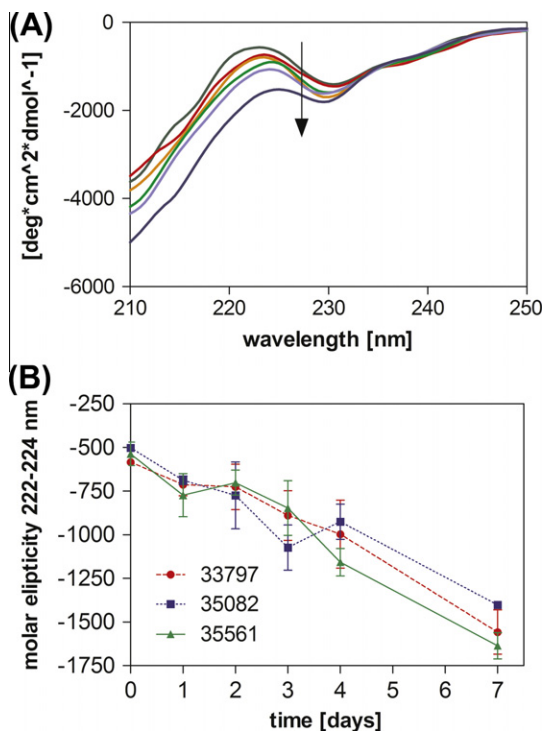


Fig. 6. Far UV CD spectra of batch 33797 (A) and maximum far-UV CD signals recorded as the average signal from 222 to 224 nm of batches 33797, 35082, and 35561 in the progress of the stress study at 50 °C (B). (For interpretation of the references to color in this figure legend, the reader is referred to the web version of this article.)

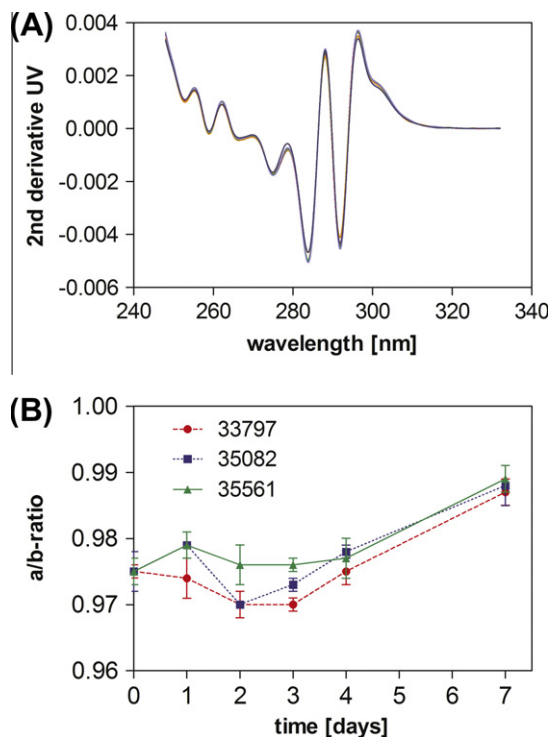


Fig. 7. Second derivative UV spectra of batch 33797 (A) and a/b-ratio of batches 33797, 35082, and 35561 in the progress of the stress study at 50 °C (B). (For interpretation of the references to color in this figure legend, the reader is referred to the web version of this article.)

stress study (Fig. 7B). Only after 7 days, a minor significant increase in the a/b-ratio was measured for all three batches, pointing to a shift towards a more polar microenvironment of the tyrosine residues [23]. Altogether, second derivative UV spectroscopy has a low sensitivity to detect conformational changes of etanercept upon thermal stress, and discrimination of the stability between batches was not possible.

3.8. Enzyme-linked immunosorbent analysis

TNF- α binding capacity after heating and subsequent aggregation of the three batches was measured by ELISA. The etanercept concentration obtained by ELISA, which is related to the binding of etanercept to its target (TNF- α), did not decline during the stress study (Fig. 8). On the contrary, it was observed that the apparent

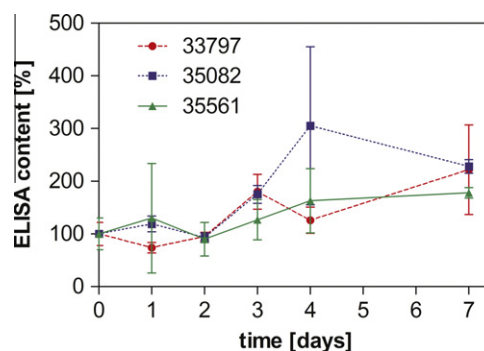


Fig. 8. TNF- α binding capacity (% of unstressed) determined by ELISA of batches 33797, 35082, and 35561 in the progress of the stress study at 50 °C. (For interpretation of the references to color in this figure legend, the reader is referred to the web version of this article.)

binding capacity increased by about 80–120% after 7 days of thermal stress. Note that the precision of the ELISA at these non-physiologically high etanercept levels is relatively poor, which limits its use as a stability-indicating method.

3.9. Statistical comparison of the sensitivity of the different methods

In order to compare the sensitivity of the different methods to stress-induced changes in the protein, the results from day 1 to 7 of the stress study were compared with the initial values for unstressed etanercept (day 0) by one-way ANOVA analysis (Table 1). The methods could be ranked according to their sensitivity to detect changes in the order Bis-ANS fluorescence > HP-SEC > DLS > Far-UV CD spectroscopy > ELISA > second derivative UV spectroscopy. No significant changes were found by light obscuration in the progress of the stress study.

Table 1

Statistical comparison of the sensitivity of the different methods to detect structural changes in etanercept.^a

Parameter	Batch	Day 1	Day 2	Day 3	Day 4	Day 7
HP-SEC, monomer	33797	ns	***	***	***	***
	35082	ns	***	***	***	***
	35561	ns	ns	**	***	***
	All batches	ns	**	***	***	***
HP-SEC, dimer	33797	*	***	***	***	***
	35082	*	**	***	***	***
	35561	**	***	***	***	***
	All batches	**	***	***	***	***
HP-SEC, HMW	33797	ns	**	***	***	***
	35082	ns	ns	***	***	***
	35561	ns	**	***	***	***
	All batches	ns	*	***	***	***
DLS, Zave	33797	ns	ns	ns	*	***
	35082	ns	ns	**	***	***
	35561	ns	ns	ns	*	***
	All batches	ns	ns	***	***	***
DLS, PDI	33797	ns	ns	ns	ns	ns
	35082	ns	ns	ns	ns	ns
	35561	ns	ns	*	ns	ns
	All batches	ns	ns	***	***	*
LO, 1/10/25 μ m	33797	ns	ns	ns	ns	ns
	35082	ns	ns	*/ns/ns	ns	ns
	35561	ns	ns	ns	ns	ns
	All batches	ns	ns	ns/ns/**	ns	ns
Bis-ANS	33797	**	***	***	***	***
	35082	***	***	***	***	***
	35561	*	**	***	***	***
	All batches	***	***	***	***	***
CD	33797	ns	ns	ns	ns	**
	35082	ns	ns	*	***	***
	35561	ns	ns	*	*	**
	All batches	*	ns	***	***	***
UV, a/b-ratio	33797	ns	ns	ns	ns	**
	35082	ns	ns	ns	ns	***
	35561	ns	ns	ns	ns	*
	All batches	ns	ns	ns	ns	***
ELISA	33797	ns	ns	ns	ns	*
	35082	ns	ns	ns	*	ns
	35561	ns	ns	ns	*	ns
	All batches	ns	ns	ns	*	***

ns = not significant.

^a Results from day 1 to 7 were compared with the results from (day 0) for each listed parameter, using one-way ANOVA analysis on each individual batch and on the three batches together.

* $p < 0.05$.

** $p < 0.01$.

*** $p < 0.001$.

The increase in Bis-ANS fluorescence compared to day 0 was statistically significant already at day 1 of the stress study for all batches, showing that this method was most sensitive. Changes in the dimer content according to HP-SEC were also significant at day 1, however, with higher p -values when compared to Bis-ANS fluorescence. Monomer and HMW content determined by HP-SEC were first at day 2 significantly different from the initial values at day 0. The next sensitive parameter was the Z-average size obtained by DLS, where changes were significant at day 3. Far-UV CD spectroscopy showed different results for the batches, with significant differences after 3 days (batches 35082 and 35561) and after 7 days (batch 33797). ELISA revealed significant changes after 4 days. The a/b -ratio obtained by second derivative UV spectroscopy was significantly different from the initial value only at day 7 of the stress study.

4. Discussion

A set of analytical methods was compared for their capability to detect structural changes and various types of aggregation in etanercept during a 1 week stress study at 50 °C, as well as to identify batch-to-batch variations. Detection of chemical changes or variations in the primary sequence of the protein was not specifically addressed within our study. The methods were selected to detect the formation of aggregates of various sizes (HP-SEC and SDS-PAGE for small aggregates, DLS for the nanometer range, and light obscuration for the micrometer size range), structural changes (Bis-ANS fluorescence, Far-UV CD spectroscopy, second derivative UV spectroscopy) and changes in TNF- α binding capacity (ELISA). When comparing the different methods for their stability-indicating properties, it is important to consider the type of instability or degradation product each method is sensitive to and at which stage of protein degradation this instability can be detected first.

For etanercept, the formation of soluble aggregates (HP-SEC, DLS), which were in part covalent (SDS-PAGE), and structural changes (Bis-ANS, far-UV CD, 2nd derivative UV spectroscopy) have been measured during the stress study. HP-SEC allows separation and quantification of monomer, dimer and higher molecular weight aggregates up to a size of about 7×10^6 Da. DLS covers a wider size range (1–1000 nm); however, quantitative analysis, as well as a separation between monomer and dimer, cannot be achieved.

According to the Lumry–Eyring model for protein aggregation [5], the equation $N \leftrightarrow TS \rightarrow A$ applies. The native protein (N) is expected to undergo reversible conformational changes into a transition state (TS) often referred to as molten globular state [29]. This transition state functions as trigger for non-native aggregation [4,5,30], because of increased exposure of hydrophobic parts, previously embedded in the core of the native protein [13]. Aggregates (A) will subsequently form, which can further develop to subvisible and visible particles.

A sensitive detection of partially folded intermediates (TS) could be useful for the early-stage analysis of protein instability. Several non-covalent fluorescent dyes possess the ability to interact with the exposed hydrophobic parts in partially unfolded proteins [31], making it possible to detect early conformational changes. Additionally, the sensitivity of extrinsic dyes for certain protein aggregates is very high, and it is possible to detect trace amounts of aggregates in the nanomolar range [32]. One of these dyes, Bis-ANS, binds to protein through hydrophobic and electrostatic interactions [33]. The increase in dye fluorescence upon interaction with TS or aggregates can be ascribed to the inhibition of the essentially non-fluorescent twisted intramolecular charge transfer state in hydrophobic environments [34,35]. Within the presented study, Bis-ANS was indeed most sensitive to detect

early-stage changes of etanercept (Table 1). However, Bis-ANS fluorescence alone does not provide information about the nature and extent of the detected instability. Therefore, additional methods are required to clarify the relation between increased dye fluorescence, conformational changes and/or aggregation.

For this purpose, we used HP-SEC (Fig. 1), SDS-PAGE (Fig. 2), DLS (Fig. 3) and light obscuration (Fig. 4), which can detect various types of aggregates ranging from small soluble aggregates to sub-visible and visible particles in the μm range. Light obscuration had no stability-indicating properties within our study, as particle formation was not a prevalent instability mechanism. However, the formation of (sub)visible particles can be considered as protein dependent and is also related to the stress method applied. Light obscuration has previously been shown to be a useful tool for detecting freeze-thawing-induced particle formation [13] or particle formation induced during mechanical stress testing [36] of monoclonal IgG antibodies.

The enhanced Bis-ANS fluorescence indicates that etanercept underwent conformational changes during the stress study, which was confirmed by Far-UV CD spectroscopy (Fig. 6) and, at a later stage, second derivative UV spectroscopy (Fig. 7). Etanercept is a fusion protein composed of the TNF- α receptor and the Fc domain of human IgG1 [18]. Both components have to be considered when evaluating the far-UV CD signal. The local minimum at 230 nm and the local maximum at 223 nm both at negative ellipticity were recognized by Liu et al. as far-UV CD signals from the Fc domain from human IgG1 [37]. The change in the position of the local maximum from 220 nm to 210 nm might be explained as a result of the formation of β -turns (local maximum at approximately 223 nm) and an incline in unordered structures [26].

The a/b -ratio determined by second derivative UV spectroscopy (Fig. 8) is rather insensitive to early changes (before day 7) and therefore less practical than Bis-ANS and far-UV CD spectroscopy to monitor early structural changes. The magnitude of the changes in a/b -ratio has been described to be in the order of 0.03–1.4 in the literature [27]. The changes seen in our study are lower than this (0.01). In a preliminary study, heating of batch 35082 was continued for more than 2 weeks (data not shown), with the a/b -ratio increasing steadily until it reached 1.02 (a change of 0.07), indicating that the trend of an increasing a/b -ratio is a sign of progressive unfolding and aggregation.

ELISA has been used to gain insight into the TNF- α binding capacity of etanercept during the stress study. An apparent increase in concentration by about 80–120% at day 7 was measured by ELISA. By this time, as seen from results obtained by HP-SEC (Fig. 1D), HMW compounds comprised 39–52% of the etanercept molecules. The ELISA data suggest that these aggregates might contain preserved TNF- α binding sites exposed at the exterior of the aggregates. Multiple functional binding sites per aggregate would lead to high avidity binding to the TNF- α molecules on the ELISA plate and thereby could explain the increase in apparent binding capacity.

Concerning the mechanism of etanercept instability under the conditions studied, we propose that a first structural change related to an increased hydrophobicity (obvious from Bis-ANS fluorescence) was followed by the formation of structurally changed (Bis-ANS fluorescence, Far-UV CD) protein and soluble aggregates (DLS, HP-SEC).

Within the study, three different batches of Enbrel® 50 mg ($n = 3$ each) were included. Before applying thermal stress, none of the analytical methods used was capable of detecting differences in quality between the batches. The stress study revealed that batch 33797 was less stable than batch 35561 and batch 35082, as detected by HP-SEC, DLS, Bis-ANS fluorescence. However, the observed differences were minor and should not be overestimated. A possible explanation could be that batch 33797 had an earlier

expiry date than the other batches. Therefore, etanercept in this batch might be already more perturbed as compared with the newer batches. However, also differences in the (partly unknown) history of the batches with respect to transport and storage might play a role. HP-SEC, DLS and Bis-ANS fluorescence were not only found to be most sensitive to detect changes of etanercept during the thermal stress study at an early time point, but were also most suitable to distinguish differences between the batches with respect to their resistance to heat stress.

5. Conclusion

The applied analytical methods could be ranked according to their sensitivity to detect instability of etanercept at an early stage during stress testing at 50 °C in the order Bis-ANS fluorescence > HP-SEC > DLS > Far-UV CD > ELISA > second derivative UV spectroscopy. Light obscuration revealed no significant changes during the stress study. To judge the comparison of the methods within the study, it is important to consider the type of instability each method probes and at which stage of protein degradation this instability can be detected first. In the progress of the stability study, the changes detected by Bis-ANS correlated well to a loss in monomer and concomitant aggregation (HP-SEC, DLS) as well as conformational changes (far-UV CD, second derivative UV spectroscopy). ELISA pointed at increased TNF- α binding capacity of etanercept following aggregation in the thermally stressed samples, but its poor precision makes it less suitable as stability-indicating method.

Acknowledgement

This research is supported by the Dutch Technology Foundation STW, applied science division of NWO and the Technology Program of the Ministry of Economic Affairs.

References

- [1] D.J. Crommelin, G. Storm, R. Verrijck, L. de Leede, W. Jiskoot, W.E. Hennink, Shifting paradigms: biopharmaceuticals versus low molecular weight drugs, *Int. J. Pharm.* 266 (2003) 3–16.
- [2] G. Walsh, Biopharmaceutical benchmarks 2006, *Nat. Biotechnol.* 24 (2006) 769–776.
- [3] M.C. Manning, D.K. Chou, B.M. Murphy, R.W. Payne, D.S. Katayama, Stability of protein pharmaceuticals: an update, *Pharm. Res.* 27 (2010) 544–575.
- [4] W. Wang, S. Nema, D. Teagarden, Protein aggregation – pathways and influencing factors, *Int. J. Pharm.* 390 (2010) 89–99.
- [5] E.Y. Chi, S. Krishnan, T.W. Randolph, J.F. Carpenter, Physical stability of proteins in aqueous solution: mechanism and driving forces in nonnative protein aggregation, *Pharm. Res.* 20 (2003) 1325–1336.
- [6] S. Hermeling, D.J. Crommelin, H. Schellekens, W. Jiskoot, Structure–immunogenicity relationships of therapeutic proteins, *Pharm. Res.* 21 (2004) 897–903.
- [7] A.S. Rosenberg, Effects of protein aggregates: an immunologic perspective, *AAPS J.* 8 (2006) E501–507.
- [8] H. Schellekens, Immunogenicity of therapeutic proteins: clinical implications and future prospects, *Clin. Ther.* 24 (2002) 1720–1740, discussion 1719.
- [9] N. Jeandidier, S. Boivin, R. Sapin, F. Rosart-Ortega, B. Uring-Lambert, P. Reville, M. Pinget, Immunogenicity of intraperitoneal insulin infusion using programmable implantable devices, *Diabetologia* 38 (1995) 577–584.
- [10] D.C. Robbins, S.M. Cooper, S.E. Fineberg, P.M. Mead, Antibodies to covalent aggregates of insulin in blood of insulin-using diabetic patients, *Diabetes* 36 (1987) 838–841.
- [11] W.V. Moore, P. Leppert, Role of aggregated human growth hormone (hGH) in development of antibodies to hGH, *J. Clin. Endocrinol. Metab.* 51 (1980) 691–697.
- [12] M.M. van Beers, W. Jiskoot, H. Schellekens, On the role of aggregates in the immunogenicity of recombinant human interferon beta in patients with multiple sclerosis, *J. Interferon. Cytokine Res.* 30 (2010) 767–775.
- [13] A. Hawe, J.C. Kasper, W. Friess, W. Jiskoot, Structural properties of monoclonal antibody aggregates induced by freeze-thawing and thermal stress, *Eur. J. Pharm. Sci.* 38 (2009) 79–87.
- [14] H.C. Mahler, W. Friess, U. Grauschopf, S. Kiese, Protein aggregation: pathways, induction factors and analysis, *J. Pharm. Sci.* 98 (2009) 2909–2934.

- [15] A. Hawe, W. Friess, M. Sutter, W. Jiskoot, Online fluorescent dye detection method for the characterization of immunoglobulin G aggregation by size exclusion chromatography and asymmetrical flow field flow fractionation, *Anal. Biochem.* 378 (2008) 115–122.
- [16] J.F. Carpenter, T.W. Randolph, W. Jiskoot, D.J. Crommelin, C.R. Middaugh, G. Winter, Potential inaccurate quantitation and sizing of protein aggregates by size exclusion chromatography: essential need to use orthogonal methods to assure the quality of therapeutic protein products, *J. Pharm. Sci.* 99 (2010) 2200–2208.
- [17] J. den Engelsman, P. Garidel, R. Smulders, H. Koll, B. Smith, S. Bassarab, A. Seidl, O. Hainzl, W. Jiskoot, Strategies for the assessment of protein aggregates in pharmaceutical biotech product development, *Pharm. Res.* (2010).
- [18] Amgen/Wyeth, Enbrel, full prescription information, 09/2009.
- [19] M.M. Goldenberg, Etanercept, a novel drug for the treatment of patients with severe, active rheumatoid arthritis, *Clin. Ther.* 21 (1999) 75–87. discussion 71–72.
- [20] X.C. Yu, W. Margolin, Inhibition of assembly of bacterial cell division protein FtsZ by the hydrophobic dye 5,5'-bis-(8-anilino-1-naphthalenesulfonate), *J. Biol. Chem.* 273 (1998) 10216–10222.
- [21] A. Aghaie, A.A. Pourfathollah, S.Z. Bathaie, S.M. Moazzeni, H.K. Pour, S. Banazadeh, Structural study on immunoglobulin G solution after pasteurization with and without stabilizer, *Transfus. Med.* 18 (2008) 62–70.
- [22] S.M. Kelly, T.J. Jess, N.C. Price, How to study proteins by circular dichroism, *Biochim. Biophys. Acta* 1751 (2005) 119–139.
- [23] R. Ragone, G. Colonna, C. Balestrieri, L. Servillo, G. Irace, Determination of tyrosine exposure in proteins by second-derivative spectroscopy, *Biochemistry* 23 (1984) 1871–1875.
- [24] M.K. de Vries, I.E. van der Horst-Bruinsma, M.T. Nurmohamed, L.A. Aarden, S.O. Stapel, M.J. Peters, J.C. van Denderen, B.A. Dijkmans, G.J. Wolbink, Immunogenicity does not influence treatment with etanercept in patients with ankylosing spondylitis, *Ann. Rheum. Dis.* 68 (2009) 531–535.
- [25] Ph. Eur., General Chapter 2.9.19. Particulate contamination: sub-visible particles, in: *European Pharmacopoeia*, sixth ed., 2010.
- [26] M. Bloemendal, W. Jiskoot, Circular dichroism spectroscopy, in: W. Jiskoot, D.J.A. Crommelin (Eds.), *Methods for Structural Analysis of Protein Pharmaceuticals*, APPS Press, Arlington, 2005, pp. 83–129.
- [27] L.A. Kueltszo, C.R. Middaugh, Ultraviolet absorption spectroscopy, in: W. Jiskoot, D.J.A. Crommelin (Eds.), *Methods for Structural Analysis of protein Pharmaceuticals*, APPS Press, Arlington, 2005, pp. 1–26.
- [28] H. Mach, C.R. Middaugh, Simultaneous monitoring of the environment of tryptophan, tyrosine, and phenylalanine residues in proteins by near-ultraviolet second-derivative spectroscopy, *Anal. Biochem.* 222 (1994) 323–331.
- [29] V.S. Pande, D.S. Rokhsar, Is the molten globule a third phase of proteins?, *Proc Natl. Acad. Sci. USA* 95 (1998) 1490–1494.
- [30] J.S. Philo, T. Arakawa, Mechanisms of protein aggregation, *Curr. Pharm. Biotechnol.* 10 (2009) 348–351.
- [31] A. Hawe, M. Sutter, W. Jiskoot, Extrinsic fluorescent dyes as tools for protein characterization, *Pharm. Res.* 25 (2008) 1487–1499.
- [32] M. Sutter, S. Oliveira, N.N. Sanders, B. Lucas, A. van Hoek, M.A. Hink, A.J. Visser, S.C. De Smedt, W.E. Hennink, W. Jiskoot, Sensitive spectroscopic detection of large and denatured protein aggregates in solution by use of the fluorescent dye Nile red, *J. Fluoresc.* 17 (2007) 181–192.
- [33] A. Bothra, A. Bhattacharyya, C. Mukhopadhyay, K. Bhattacharyya, S. Roy, A fluorescence spectroscopic and molecular dynamics study of bis-ANS/protein interaction, *J. Biomol. Struct. Dyn.* 15 (1998) 959–966.
- [34] T.L. Chang, H.C. Cheung, A model for molecules with twisted intramolecular charge transfer characteristics: solvent polarity effect on the nonradiative rates of dyes in a series of water–ethanol mixed solvents, *Chem. Phys. Lett.* 173 (1990) 343–348.
- [35] K. Das, N. Sarkar, D. Nath, K. Bhattacharya, Non-radiative pathways of anilino-naphthalene sulphonates: twisted intramolecular charge transfer versus intersystem crossing, *Spectrochim. Acta A Mol. Biomol. Spectrosc.* 48A (1992) 1701–1705.
- [36] H.C. Mahler, R. Muller, W. Friess, A. Delille, S. Matheus, Induction and analysis of aggregates in a liquid IgG1-antibody formulation, *Eur. J. Pharm. Biopharm.* 59 (2005) 407–417.
- [37] D. Liu, D. Ren, H. Huang, J. Dankberg, R. Rosenfeld, M.J. Cocco, L. Li, D.N. Brems, R.L. Remmele Jr., Structure and stability changes of human IgG1 Fc as a consequence of methionine oxidation, *Biochemistry* 47 (2008) 5088–5100.